

The following resources related to this article are available online at www.sciencemag.org (this information is current as of July 17, 2009):

Updated information and services, including high-resolution figures, can be found in the online version of this article at:

<http://www.sciencemag.org/cgi/content/full/325/5938/318>

Supporting Online Material can be found at:

<http://www.sciencemag.org/cgi/content/full/325/5938/318/DC1>

A list of selected additional articles on the Science Web sites **related to this article** can be found at:

<http://www.sciencemag.org/cgi/content/full/325/5938/318#related-content>

This article **cites 30 articles**, 14 of which can be accessed for free:

<http://www.sciencemag.org/cgi/content/full/325/5938/318#otherarticles>

This article appears in the following **subject collections**:

Genetics

<http://www.sciencemag.org/cgi/collection/genetics>

Information about obtaining **reprints** of this article or about obtaining **permission to reproduce this article** in whole or in part can be found at:

<http://www.sciencemag.org/about/permissions.dtl>

movement in air or water, and that organisms can exploit the solid and fluidlike properties of these media to move effectively within them.

References and Notes

- R. M. Alexander, *Principles of Animal Locomotion* (Princeton Univ. Press, Princeton, NJ, 2003).
- M. H. Dickinson *et al.*, *Science* **288**, 100 (2000).
- S. Vogel, *Life in Moving Fluids* (Princeton Univ. Press, Princeton, NJ, 1994).
- E. R. Trueman, *J. Exp. Biol.* **53**, 701 (1970).
- C. R. Darwin, *The Formation of Vegetable Mould, Through the Action of Worms: With Observations on Their Habits* (John Murray, London, 1881).
- K. Dorgan, P. Jumars, B. Johnson, B. Boudreau, E. Landis, *Nature* **433**, 475 (2005).
- G. Lauder, E. Drucker, *Physiology (Bethesda)* **17**, 235 (2002).
- F. Meysman, J. Middelburg, C. Heip, *Trends Ecol. Evol.* **21**, 688 (2006).
- E. Arnold, *J. Zool.* **235**, 351 (1995).
- C. White, *Aust. J. Zool.* **49**, 663 (2001).
- E. Ezcurra, *Global Deserts Outlook* (United Nations Environmental Programme, Nairobi, Kenya, 2006).
- H. M. Jaeger, S. R. Nagel, R. P. Behringer, *Phys. Today* **49**, 32 (1996).
- W. W. Dickinson, J. D. Ward, *J. Sediment. Res. Sect. A* **64**, 226 (1994).
- R. Nedderman, *Statics and Kinematics of Granular Materials* (Cambridge Univ. Press, New York, 1992).
- C. Li, P. B. Umbanhowar, H. Komsuoglu, D. E. Koditschek, D. I. Goldman, *Proc. Natl. Acad. Sci. U.S.A.* **106**, 3029 (2009).
- W. Baumgartner *et al.*, *J. Bionic Eng.* **4**, 1 (2007).
- C. Gans, *Integr. Comp. Biol.* **15**, 455 (1975).
- W. Baumgartner *et al.*, *PLoS One* **3**, (e3309), 1 (2008).
- Materials and methods are available as supporting material on Science Online.
- A. A. Biewener, G. B. Gillis, *J. Exp. Biol.* **202**, 3387 (1999).
- J. Gray, H. Lissman, *J. Exp. Biol.* **41**, 135 (1964).
- J. Korta, D. Clark, C. Gabel, L. Mahadevan, A. Samuel, *J. Exp. Biol.* **210**, 2383 (2007).
- J. Gray, G. J. Hancock, *J. Exp. Biol.* **32**, 802 (1955).
- I. Albert *et al.*, *Phys. Rev. E Stat. Nonlin. Soft Matter Phys.* **64**, 61303 (2001).
- R. Albert, M. Pfeifer, A. Barabási, P. Schiffer, *Phys. Rev. Lett.* **82**, 205 (1999).
- K. Wieghardt, *Annu. Rev. Fluid Mech.* **7**, 89 (1975).
- A. N. Schofield, C. P. Wroth, *Critical State Soil Mechanics* (McGraw-Hill, London, 1968).
- B. R. Moon, C. Gans, *J. Exp. Biol.* **201**, 2669 (1998).
- This work was supported by NSF Physics of Living Systems grant PHY-0749991 and the Burroughs Wellcome Fund. We thank R. Full and T. Papenfuss for helpful discussion. We thank S. Steinmetz and N. Gravish for experimental assistance and P. Umbanhowar for discussion of the drag model and careful reading of the manuscript.

Supporting Online Material

www.sciencemag.org/cgi/content/full/325/5938/314/DC1

Materials and Methods

Figs. S1 to S3

Table S1

References

Movies S1 to S3

18 February 2009; accepted 5 June 2009

10.1126/science.1172490

Targeted Retrieval and Analysis of Five Neandertal mtDNA Genomes

Adrian W. Briggs,^{1*} Jeffrey M. Good,¹ Richard E. Green,¹ Johannes Krause,¹ Tomislav Maricic,¹ Udo Stenzel,¹ Carles Lalueza-Fox,² Pavao Rudan,³ Dejana Brajković,⁴ Željko Kučan,³ Ivan Gušić,³ Ralf Schmitz,^{5,6} Vladimir B. Doronichev,⁷ Liubov V. Golovanova,⁷ Marco de la Rasilla,⁸ Javier Fortea,⁸ Antonio Rosas,⁹ Svante Pääbo¹

Analysis of Neandertal DNA holds great potential for investigating the population history of this group of hominins, but progress has been limited due to the rarity of samples and damaged state of the DNA. We present a method of targeted ancient DNA sequence retrieval that greatly reduces sample destruction and sequencing demands and use this method to reconstruct the complete mitochondrial DNA (mtDNA) genomes of five Neandertals from across their geographic range. We find that mtDNA genetic diversity in Neandertals that lived 38,000 to 70,000 years ago was approximately one-third of that in contemporary modern humans. Together with analyses of mtDNA protein evolution, these data suggest that the long-term effective population size of Neandertals was smaller than that of modern humans and extant great apes.

Currently, DNA sequences determined from multiple Neandertals are restricted to short fragments [120 to 360 base pairs (bp)] of the hypervariable regions (HVRs) of mitochondrial DNA (mtDNA) (1, 2). These data have demonstrated that Neandertal mtDNA is distinct from that of modern humans (3). However, collecting sequence data from the rest of the mtDNA ge-

nome has proven difficult due to numerous technological difficulties (4). Recently, the complete mtDNA genome sequence of a ~38,000-year-old Neandertal individual from Vindija Cave, Croatia, was determined by high-throughput shotgun sequencing from total DNA extract (5). A similar approach has been used to recover complete mtDNA sequences from permafrost-preserved mammoths and a human (6, 7). However, the amount of shotgun sequencing needed to retrieve complete mtDNA sequences is prohibitive for most ancient bone specimens due to the high fraction of environmental DNA that they contain. For example, only 0.001% of DNA sequences determined from typical well-preserved Neandertal specimens are derived from mtDNA (table S1). Thus, a simple shotgun approach would require hundreds or thousands of high-throughput pyrosequencing runs to recover a single Neandertal mitochondrial genome (table S1). Direct polymerase chain reaction (PCR) is also poorly suited for retrieving complete Neandertal mtDNA genomes, because DNA extracted from the fossils

is so fragmented that hundreds of overlapping amplicons would be necessary, either requiring highly multiplexed primer mixes that present severe difficulties for avoiding modern human contamination, or many parallel amplification reactions that consume large amounts of precious ancient DNA extracts (8).

We have developed a method—primer extension capture (PEC)—that directly isolates specific DNA sequences from complex libraries of highly degraded DNA (Fig. 1). PEC uses 5'-biotinylated oligonucleotide primers and a DNA polymerase to capture specific target sequences from an adaptor-ligated DNA library. It combines the high specificity of PCR primers with the numerous advantages of a library sequencing approach, including immortalization through reamplification from adaptor priming sites (9) (fig. S1), contamination control with project-specific barcodes (5, 10), access to very short fragments predominant in ancient extracts (11), and quantification of the number of unique ancient DNA molecules, which is necessary to identify nucleotide misincorporations (10–12).

We used PEC to recover the entire Neandertal mtDNA genome [supporting online material (SOM)] of five individuals from four sites across the geographic range of Neandertals (Fig. 2 and table S2). One individual (Vindija 33.25) from Vindija Cave, Croatia, is undated but was found in an older stratigraphic layer than the previously sequenced bone (5) (Vindija 33.16), which was dated to ~38,000 years before present (yr B.P.) (3). Two individuals (Feldhofer 1 and 2, the former being the Neandertal type specimen) come from Kleine Feldhofer Grotte, Neander Valley, Germany, and are dated to ~40,000 yr B.P. (13). One individual (Sidron 1253) comes from El Sidron Cave, Spain, and is dated to ~39,000 yr B.P. (14), and one (Mezmaiskaya 1) comes from Mezmaiskaya Cave, Russia, and is dated to 60,000 to 70,000 yr B.P. (15).

We generated between 170,330 and 521,680 sequence reads per individual on the 454 FLX platform and processed them with a mapping

¹Max-Planck Institute for Evolutionary Anthropology, D-04103 Leipzig, Germany. ²Institute of Evolutionary Biology, Consejo Superior de Investigaciones Científicas, Universitat Pompeu Fabra, 08003 Barcelona, Spain. ³Croatian Academy of Sciences and Arts, Zrinski trg 11, HR-10000 Zagreb, Croatia. ⁴Croatian Academy of Sciences and Arts, Institute for Quaternary Paleontology and Geology, Ante Kovačića 5, HR-10000 Zagreb, Croatia. ⁵Landschaftsverband Rheinland Landesmuseum, D-53115 Bonn, Germany. ⁶Department of Early Prehistory and Quaternary Ecology, University of Tübingen, Germany. ⁷Laboratory of Prehistory, St. Petersburg, Russia. ⁸Área de Prehistoria Departamento de Historia Universidad de Oviedo, Oviedo, Spain. ⁹Departamento de Paleobiología, Museo Nacional de Ciencias Naturales, Consejo Superior de Investigaciones Científicas, Madrid, Spain.

*To whom correspondence should be addressed. E-mail: briggs@eva.mpg.de

assembly program (SOM), taking the Vindija 33.16 mtDNA sequence (5) as a reference. Between 18.2 and 40.2% of sequences were identified as mitochondrial, representing a raw target enrichment of 3640- to 80,400-fold (table S1). Nontarget sequences were enriched in sequence motifs from the 3' ends of PEC primers (fig. S2), suggesting the occurrence of some false priming events. All five individuals showed continuous coverage across the entire mtDNA genome with an average unique read depth of 18.0 to 56.3 \times (fig. S3). As reported previously for Neandertal mtDNA (5), average fragment lengths were short (51.3 to 79.3 bp, fig. S4), coverage was positively correlated with GC content (fig. S5), and bases differing from the consensus were dominated by C/G \rightarrow T/A substitutions (fig. S6), consistent with deamination of cytosine (10, 11, 16) clustered toward the ends of fragments (10, 11) (fig. S7). However, the rate of C/G \rightarrow T/A misincorporations varied among the fossils and was negatively correlated with average fragment length (fig. S8), likely reflecting differential hydrolytic damage suffered by DNA in different depositional environments. To determine if sequencing coverage in each assembly was sufficient to overcome misincorporations and other sequencing errors, we calculated the proportion of reads at each position that matched the assembly consensus base (fig. S9). Apart from a single ambiguous position (see fig. S10 for resolution of this position), support across the 82,865 aligned positions (five 16,565-bp mtDNA genomes) was high (mean = 98.5%, minimum 60.0%). At all 43 positions with support lower than 75%, we observed a minor base consistent with deamination of cytosine. Sites that differed from the Neandertal reference had coverage (mean = 32.0 \times) and support (mean = 98.7%) similar to those that matched the reference (mean coverage = 36.5 \times ; mean support = 98.5%). None of these sites had support lower than 78% (table S3), and their locations were not correlated with PEC primer sites (all $P > 0.50$, Fisher's exact test; table S4). These data suggest that the five consensus sequences are unlikely to have been affected by sequencing or base damage errors, because such errors would tend to create sequence differences that would be poorly supported and located in regions of low coverage.

We quantified the level of modern human DNA contamination in each of our assemblies by counting Neandertal versus contaminating fragments at all positions (124 to 130 positions per individual) where the Neandertal was found to differ from a worldwide panel of 311 aligned modern human mtDNA genomes (5). From 876 to 2969 fragments overlapping these positions per Neandertal assembly, we estimated that modern human contamination ranged from 0.2 to 1.4% (table S5). At these levels, contamination is highly unlikely to affect the determination of consensus sequences. Finally, the PEC-derived Neandertal mtDNA genomes were compared to PCR-amplified HVR sequences from the same individuals (13, 17) (SOM and fig. S11). Aligned sequences were iden-

tical between the two methods for every individual except Feldhofer 1, where some previously postulated errors for PCR-derived positions (13) were confirmed as such by PEC.

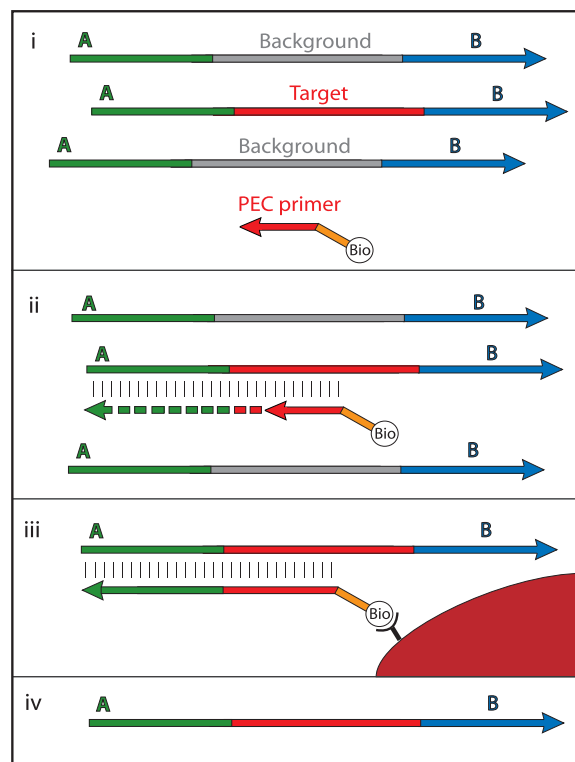
Comparison among the six complete Neandertal mtDNA genomes revealed a total of 55 variable positions across 16,565 aligned nucleotides (Table 1). On average, the six Neandertal mtDNAs differ by 20.4 substitutions. We contrasted Neandertal mtDNA diversity with variation among modern humans as represented by the revised Cambridge reference sequence (18) and a previously published worldwide sample of 53 individuals (19). Variation among the Neandertals was approximately one-third of that estimated for modern humans worldwide, approximately half that of individuals from non-African populations, and similar to that of the nine Europeans in this sample (Table 1). When compared to a broader survey of 30 modern Europeans (Table 1 and SOM), Neandertals had 37% lower mtDNA diversity. Because the Neandertal sequences stem from several distinct time points spanning thousands of years, we used coalescent simulations (20, 21) to assess the magnitude of any bias introduced by the temporal sampling and found that it may cause up to a ~20% overestimate of Neandertal genetic diversity (table S6) relative to a sample drawn from a single point in time. Thus, the observation that mtDNA diversity is lower in Neandertals than in modern humans appears to be conservative with respect to sampling over time.

Estimation of phylogenetic relationships confirmed the reciprocally monophyletic status of Neandertal and modern human mtDNAs (Fig. 2). Among the six Neandertal mtDNAs, the sequence

from Mezmaiskaya is more divergent from the other five (44.4 mean pairwise differences) than the latter are among themselves (8.4 mean pairwise differences). As observed previously (5), the Neandertal branch in the phylogeny appears shorter than that of modern humans. Simulations show that this asymmetry is well within the expected range of stochastic variation given that the Neandertal mtDNA sequences are at least 38,000 years old (fig. S12).

With a Bayesian approach (22) calibrated with the fossil ages of the five dated Neandertal sequences and a human-chimpanzee divergence of ~6 million years (see SOM), we estimated the time to the most recent common Neandertal mtDNA ancestor to be ~109,800 yr B.P. [84,630 to 138,500 yr B.P., 95% highest posterior density (HPD); table S7]. This is ~80% of the mean coalescent time estimated for modern human mtDNA with the same approach (mean time to the most recent common ancestor = 136,100 yr B.P.; 94,930 to 178,700, 95% HPD). Assuming that positive selection has not influenced Neandertal mtDNA variation, a recent coalescent time despite a ~38,000-year truncation of the Neandertal lineage suggests that the effective population size of Neandertals (N_e) was small and probably included fewer than 3500 females (mean $N_e = 1476$; 268 to 3510, 95% HPD). The recovery of identical mtDNA sequences from Vindija in Croatia and the Neander Valley in Germany, which are more than 850 km apart, supports the inference of a small effective population size in Neandertals. Given the temporal sampling and a constant effective size of 1500, the probability of sampling at least two identical mtDNA genomes among six is reasonably high ($P = 0.25$). In contrast,

Fig. 1. Primer extension capture (PEC). (i) 5'-Biotinylated oligonucleotide primers (PEC primers) are added to a 454 library [in which the A and B adaptor molecules carry a project-specific barcode (10)] and are allowed to anneal to their respective target sequences. (ii) A single *Taq* DNA polymerase extension step is performed, resulting in a double-stranded association between primer and target that includes the 5' adaptor sequence. (iii) Excess PEC primers are removed by spin column purification, and the biotinylated primer:target duplexes are captured by streptavidin-coated magnetic beads. The beads are washed stringently above the melting temperature of the PEC primers, to ensure that templates upon which extension occurred will preferentially remain associated with the primers. (iv) Captured and washed targets are eluted from the beads, amplified with adaptor priming sites, and subjected either to a second round of extension and capture or directly to 454 emulsion PCR (full details are in the SOM).



only one pair of identical sequences was identified among the 30 Europeans, as expected given the recent population expansion of modern humans (23).

The observation that the most divergent mtDNA genome was retrieved from the oldest and easternmost individual analyzed (Mezmaiskaya 1) raises the possibility that genetic structure existed between Neandertals from different geographic regions and/or time points (1). Unaccounted-for population structure within the sample of Neandertals could inflate the estimate of effective population size (24). We therefore used PEC to retrieve a partial mtDNA genome (13,568 bp, SOM) from a second, more recent individual from Mezmaiskaya Cave [Mezmaiskaya 2, ~41,000 yr B.P. (15); table

S2]. This mtDNA sequence unambiguously groups with the five complete mtDNAs from the western sites (fig. S13). Thus, no obvious phylogeographic structure can be discerned among the seven mtDNAs analyzed. Analysis of additional individuals from different times and locations will be necessary to examine broader patterns of temporal and/or geographic variation in Neandertal genetic diversity (1).

Low mtDNA diversity may reflect a low effective population size of Neandertals over a large part of their ~400,000-year history. Alternatively, it might be typical only of late Neandertals, who may have experienced a reduction in population size due to direct or indirect influences from modern humans expanding out of Africa. Of relevance for

this question is the observation that the first complete Neandertal mtDNA genome had a higher rate of protein evolution (measured as the ratio of per site amino acid replacement to per site silent substitutions, dN/dS) than humans and great apes (5). This pattern is consistent with a long-term reduction in the effective population size of Neandertals, because purifying selection is expected to be less effective at purging weakly deleterious mutations in small populations (25). We tested this by partitioning dN/dS into polymorphic and fixed differences along both the Neandertal and modern human lineages. dN/dS for fixed differences was about twice as high along the Neandertal lineage (0.168) as along the modern human lineage (0.082; Fig. 2) or the lineages of chimpanzees and bonobos ($dN/dS < 0.08$; table S8). Furthermore, a likelihood model (26) in which dN/dS is higher in Neandertals versus the other lineages best explains patterns of protein evolution across all groups (fig. S14). Although this difference appears pronounced, our estimate is based on relatively few amino acid substitutions overall, and lineage-specific variation in dN/dS provides only an indirect assessment of long-term effective population size. Nonetheless, patterns of mtDNA protein evolution are consistent with the notion that the effective population size of Neandertals was small not only among late Neandertals but over a longer period of their existence. Clearly, the recovery of nuclear sequences from multiple Neandertals will be necessary to arrive at a more complete picture of their population history. Encouragingly, PEC and other targeted resequencing approaches (27–29) now make this feasible.

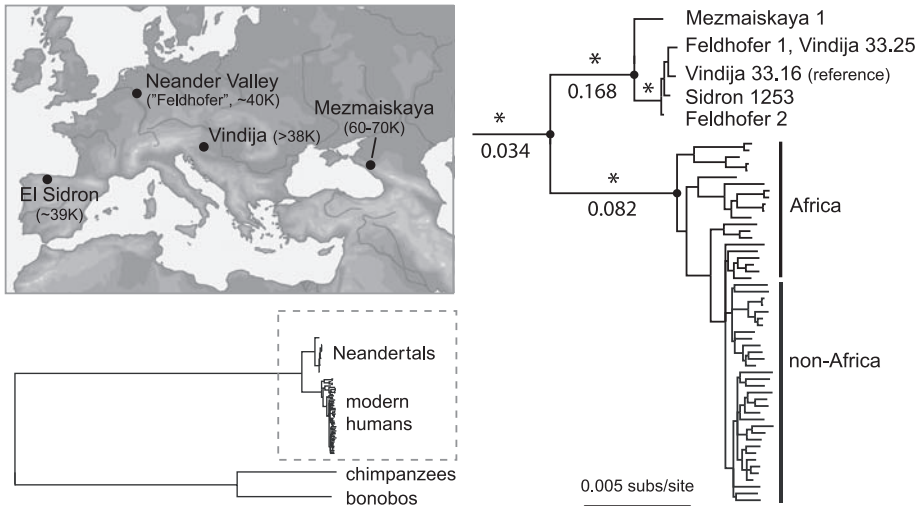


Fig. 2. mtDNA phylogeny of Neandertals and their close relatives. The top left panel gives the localities and estimated ages of the analyzed Neandertals. The phylogeny was estimated with a Bayesian approach (30) under a GTR+I+ Γ model of sequence evolution. Modern humans are represented by the revised Cambridge reference sequence and a collection of 53 sequences sampled from major language groups. Nodes marked with an asterisk (*) have a posterior probability of 1.0. For clarity, support for major partitions within modern humans is not shown. Estimates of dN/dS for 12 concatenated protein-coding genes are indicated below the branch.

Table 1. Mitochondrial DNA variation in Neandertals and modern humans.

| Sample | Length* | N† | Hap‡ | S§ | MPWD | θ_{π} (%)¶ |
|--------------------------------|---------|----|------|-----|------|---------------------|
| <i>All sites</i> | | | | | | |
| Neandertals | 16,565 | 6 | 5 | 55 | 20.4 | 0.123 |
| Modern humans | 16,547 | 54 | 54 | 658 | 60.5 | 0.365 |
| African | 16,556 | 21 | 21 | 365 | 76.5 | 0.462 |
| Non-African | 16,554 | 33 | 33 | 364 | 38.1 | 0.230 |
| European | 16,566 | 9 | 9 | 87 | 23.7 | 0.143 |
| European (expanded)# | 16,565 | 30 | 29 | 260 | 32.3 | 0.195 |
| <i>Third codon positions**</i> | | | | | | |
| Neandertals | 3,575 | 6 | 5 | 22 | 8.3 | 0.231 |
| Modern humans | 3,575 | 54 | 52 | 283 | 23.8 | 0.667 |
| African | 3,575 | 21 | 19 | 164 | 32.6 | 0.911 |
| Non-African | 3,575 | 33 | 33 | 134 | 13.5 | 0.378 |
| European | 3,575 | 9 | 9 | 23 | 5.9 | 0.165 |
| European (expanded)# | 3,575 | 30 | 29 | 91 | 10.5 | 0.293 |

*Number of aligned positions excluding alignment gaps. †Number of sequences. ‡Number of distinct mtDNA sequences (haplotypes). §Number of variable sites. ||Mean number of pairwise differences. ¶Average percentage of pairwise differences per site. #Expanded to include additional, previously published complete mtDNA genomes. See SOM for details. **Based on a 10,725-bp concatenated alignment of the 12 mtDNA genes coded on the same strand, excluding regions with overlapping reading frames.

References and Notes

1. L. Excoffier, *Curr. Biol.* **16**, R650 (2006).
2. J. Krause et al., *Nature* **449**, 902 (2007).
3. D. Serre et al., *PLoS Biol.* **2**, E57 (2004).
4. S. Paabo et al., *Annu. Rev. Genet.* **38**, 645 (2004).
5. R. E. Green et al., *Cell* **134**, 416 (2008).
6. M. T. Gilbert et al., *Proc. Natl. Acad. Sci. U.S.A.* **105**, 8327 (2008).
7. M. T. Gilbert et al., *Science* **320**, 1787 (2008).
8. C. Anderung, P. Persson, A. Bouwman, R. Elburg, A. Gotherstrom, *Forensic Sci. Int. Genet.* **2**, 104 (2008).
9. M. J. Blow et al., *Genome Res.* **18**, 1347 (2008).
10. A. W. Briggs et al., *Proc. Natl. Acad. Sci. U.S.A.* **104**, 14616 (2007).
11. P. Brotherton et al., *Nucleic Acids Res.* **35**, 5717 (2007).
12. R. Mackelprang, E. M. Rubin, *Science* **321**, 211 (2008).
13. R. W. Schmitz et al., *Proc. Natl. Acad. Sci. U.S.A.* **99**, 13342 (2002).
14. C. Lalueza-Fox et al., *Mol. Biol. Evol.* **22**, 1077 (2005).
15. A. R. Skinner et al., *Appl. Radiat. Isot.* **62**, 219 (2005).
16. M. Hofreiter, V. Jaenicke, D. Serre, A. Haeseler, V. S. Paabo, *Nucleic Acids Res.* **29**, 4793 (2001).
17. I. V. Ovchinnikov et al., *Nature* **404**, 490 (2000).
18. R. M. Andrews et al., *Nat. Genet.* **23**, 147 (1999).
19. M. Ingman, H. Kaessmann, S. Pääbo, U. Gyllenstein, *Nature* **408**, 708 (2000).
20. C. N. K. Anderson, U. Ramakrishnan, Y. L. Chan, E. A. Hadly, *Bioinformatics* **21**, 1733 (2005).
21. L. Excoffier, J. Novembre, S. Schneider, *J. Hered.* **91**, 506 (2000).
22. A. J. Drummond, A. Rambaut, *BMC Evol. Biol.* **7**, 214 (2007).
23. Q. D. Atkinson, R. D. Gray, A. J. Drummond, *Mol. Biol. Evol.* **25**, 468 (2008).

24. F. F. Jesus, J. F. Wilkins, V. N. Solferini, J. Wakeley, *Genet. Mol. Res.* **5**, 466 (2006).
 25. T. Ohta, *Nature* **246**, 96 (1973).
 26. S. L. Kosakovsky Pond, S. D. W. Frost, *Mol. Biol. Evol.* **22**, 478 (2004).
 27. A. Gnirke *et al.*, *Nat. Biotechnol.* **27**, 182 (2009).
 28. E. Hodges *et al.*, *Nat. Genet.* **39**, 1522 (2007).
 29. J. P. Noonan *et al.*, *Science* **314**, 1113 (2006).
 30. F. Ronquist, J. P. Huelsenbeck, *Bioinformatics* **19**, 1572 (2003).
 31. We thank P. Johnson, M. Knapp, A.-S. Malaspinas, M. Meyer, J. Sullivan, M. Slatkin, and anonymous reviewers

for comments; the Croatian Academy of Sciences and Arts and the Berlin-Brandenburg Academy of Sciences for logistic and scientific support; and the Presidential Innovation Fund of the Max Planck Society for financial support. The government of the Principado de Asturias funded excavations at the El Sidron site. C.L.-F. was supported by the Spanish Ministry of Education and Science and J.M.G. by an NSF international postdoctoral fellowship (OISE-0754461). Sequences are deposited at the EBI (European Bioinformatics Institute) nucleotide database with the following accession numbers: Neandertal 1 (Feldhofer 1), FM865407; Neandertal 2

(Feldhofer 2), FM865408; Sidron 1253, FM865409; Vindija 33.25, FM865410; Mezmaiskaya 1, FM865411.

Supporting Online Material

www.sciencemag.org/cgi/content/full/325/5938/318/DC1
 Materials and methods
 Figs. S1 to S14
 Tables S1 to S8
 References
 Appendix 1

3 April 2009; accepted 3 June 2009
 10.1126/science.1174462

The Human SepSecS-tRNA^{Sec} Complex Reveals the Mechanism of Selenocysteine Formation

Sotiria Palioura,¹ R. Lynn Sherrer,¹ Thomas A. Steitz,^{1,2,3} Dieter Söll,^{1,2,*} Miljan Simonović^{4*}

Selenocysteine is the only genetically encoded amino acid in humans whose biosynthesis occurs on its cognate transfer RNA (tRNA). *O*-Phosphoseryl-tRNA:selenocysteinyl-tRNA synthase (SepSecS) catalyzes the final step of selenocysteine formation by a poorly understood tRNA-dependent mechanism. The crystal structure of human tRNA^{Sec} in complex with SepSecS, phosphoserine, and thiophosphate, together with *in vivo* and *in vitro* enzyme assays, supports a pyridoxal phosphate-dependent mechanism of Sec-tRNA^{Sec} formation. Two tRNA^{Sec} molecules, with a fold distinct from other canonical tRNAs, bind to each SepSecS tetramer through their 13-base pair acceptor-T Ψ C arm (where Ψ indicates pseudouridine). The tRNA binding is likely to induce a conformational change in the enzyme's active site that allows a phosphoserine covalently attached to tRNA^{Sec}, but not free phosphoserine, to be oriented properly for the reaction to occur.

The 21st amino acid, selenocysteine (Sec), is distinct from other amino acids not only because it lacks its own tRNA synthetase, but also because it is the only one that is synthesized on the cognate tRNA in all domains of life [reviewed in (1–4)] in a process that is reminiscent of the tRNA-dependent synthesis of glu-

tamine, asparagine, and cysteine in prokaryotes (4). The importance of Sec is illustrated by the embryonic lethal phenotype of the tRNA^{Sec} knockout mouse (5) and by the presence of Sec in the active sites of enzymes involved in removing reactive oxidative species and in thyroid hormone activation (6, 7). It is intriguing that the codon for

Sec is UGA, which is normally a translational stop signal (1). During translation of selenoprotein mRNAs, UGA is recoded by the interaction of a specialized elongation factor, SelB in bacteria and EFsec in humans, with a downstream Sec-insertion sequence element that forms a stem loop (1, 3).

The first step in Sec formation involves the misacylation of tRNA^{Sec} by seryl-tRNA synthetase (SerRS) to give Ser-tRNA^{Sec} [reviewed in (3, 8)]. Although the tertiary structure of tRNA^{Sec} was unknown, it was proposed that the mischarging reaction is possible because of similarities between the tRNA^{Sec} and tRNA^{Ser} structures (3, 8). In archaea and eukaryotes, the γ -hydroxyl group of Ser-tRNA^{Sec} is subsequently phosphorylated by *O*-phosphoseryl-tRNA kinase (PSTK) (9) to give *O*-phosphoseryl-tRNA^{Sec} (Sep-tRNA^{Sec}), which is then used as a substrate for the last synthetic

¹Department of Molecular Biophysics and Biochemistry, Yale University, New Haven, CT 06520, USA. ²Department of Chemistry, Yale University, New Haven, CT 06520, USA. ³Howard Hughes Medical Institute, Yale University, New Haven, CT 06520, USA. ⁴Department of Biochemistry and Molecular Genetics, University of Illinois at Chicago, Chicago, IL 60607, USA.

*To whom correspondence should be addressed. E-mail: dieter.soll@yale.edu (D.S.); msimon5@uic.edu (M.S.)

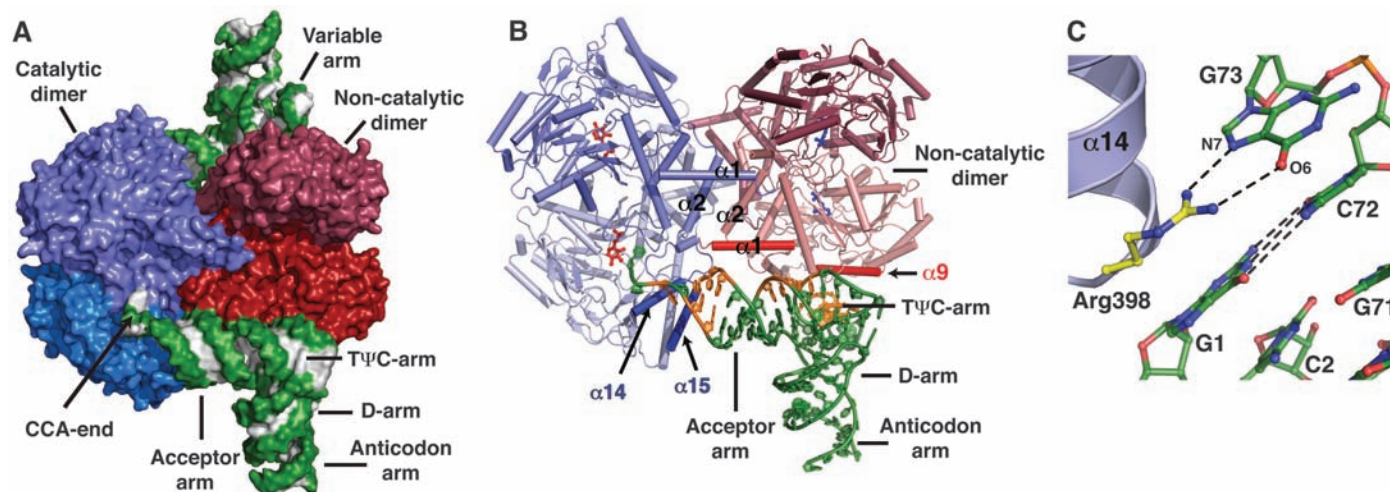


Fig. 1. Structure of human SepSecS in complex with unacylated tRNA^{Sec}. (A) Surface representation of the physiological complex of SepSecS with tRNA^{Sec}. The subunits of the catalytic dimer are dark blue, those of the noncatalytic dimer are light blue, and the backbone of tRNA^{Sec} is green and gray, respectively. (B) The catalytic dimer interacts with the acceptor arm of tRNA^{Sec} through helices α 14 and α 15

(blue). The α 1 helix (red) of the noncatalytic dimer interacts with the rest of the acceptor-T Ψ C arm. The regions of tRNA^{Sec} that interact with SepSecS are shown in orange; the rest is green. One tRNA^{Sec} molecule is shown for clarity. (C) Interactions between the discriminator base G73 and the conserved Arg³⁹⁸ in the α 14- β 11 loop. The protein side chains are gold, and tRNA^{Sec} is green.